NeuroImage 254 (2022) 119119

Contents lists available at ScienceDirect

NeuroImage

journal homepage: www.elsevier.com/locate/neuroimage

Transcranial alternating current stimulation modulates cortical processing of somatosensory information in a frequency- and time-specific manner

Andrea Fabbrini[a], Andrea Guerra[b], Margherita Giangrosso[a], Nicoletta Manzo[a,c], Giorgio Leodori[a,b], Patrizio Pasqualetti[d], Antonella Conte[a,b], Vincenzo Di Lazzaro[e], Alfredo Berardelli[a,b,*]

[a] Department of Human Neurosciences, Sapienza University of Rome, Viale dell'Università 30, Rome, 00185, Italy
[b] IRCCS Neuromed, Via Atinense 18, Pozzilli, IS 86077, Italy
[c] IRCCS San Camillo Hospital, Via Alberoni 70, Venice 30126, Italy
[d] Department of Public Health and Infectious Diseases, Sapienza University of Rome, Viale dell'Università 30, Rome 00185, Italy
[e] Unit of Neurology, Neurophysiology, Neurobiology, Department of Medicine, University Campus Bio-Medico, Via Álvaro Del Portillo 21, Rome 00128, Italy

ARTICLE INFO

Keywords:
tACS
Entrainment
Mu
Somatosensory cortex
SEP
HFO

ABSTRACT

Neural oscillations can be modulated by non-invasive brain stimulation techniques, including transcranial alternating current stimulation (tACS). However, direct evidence of tACS effects at the cortical level in humans is still limited. In a tACS-electroencephalography co-registration setup, we investigated the ability of tACS to modulate cortical somatosensory information processing as assessed by somatosensory-evoked potentials (SEPs). To better elucidate the neural substrates of possible tACS effects we also recorded peripheral and spinal SEPs components, high-frequency oscillations (HFOs), and long-latency reflexes (LLRs). Finally, we studied whether changes were limited to the stimulation period or persisted thereafter. SEPs, HFOs, and LLRs were recorded during tACS applied at individual mu and beta frequencies and at the theta frequency over the primary somatosensory cortex (S1). Sham-tACS was used as a control condition. In a separate experiment, we assessed the time course of mu-tACS effects by recording SEPs before (T0), during (T1), and 1 min (T2) and 10 min (T3) after stimulation. Mu-tACS increased the amplitude of the N20 component of SEPs compared to both sham and theta-tACS. No differences were found between sham, beta-, and theta-tACS conditions. Also, peripheral and spinal SEPs, P25, HFOs, and LLRs did not change during tACS. Finally, mu-tACS-induced modulation of N20 amplitude specifically occurred during stimulation (T1) and vanished afterwards (i.e., at T2 and T3). Our findings suggest that TACS applied at the individual mu frequency is able to modulate early somatosensory information processing at the S1 level and the effect is limited to the stimulation period.

1. Introduction

Specific subpopulations of neurons in cortical brain areas show oscillatory properties (Singer, 2018). These oscillatory activities can be modulated by non-invasive brain stimulation techniques including transcranial alternating current stimulation (tACS) (Herrmann et al., 2013; Giovanni et al., 2017), which entrains neuronal activity through the temporal alignment of endogenous rhythmical brain activity with exogenous alternating currents (Thut et al., 2011). Entrainment-related tACS effects are frequency- and time-specific, i.e., they are prominent when the stimulation frequency is resonant to the endogenous rhythm of the targeted area ('endogenous resonance principle') (Ali et al., 2013; Krause et al., 2019; Johnson et al., 2020) and occur during stimulation ('online' effects) and subsequently vanish (Johnson et al., 2020; Guerra et al., 2019; Guerra et al., 2020; Bologna et al., 2019; Pozdniakov et al., 2021).

Direct evidence of the mechanisms underlying tACS entrainment effects on cortical neurons mainly comes from *in vitro* and animal studies (Ali et al., 2013; Krause et al., 2019; Johnson et al., 2020; Ozen et al., 2010; Reato et al., 2013; Vieira et al., 2020). In humans, a possible approach to verify whether tACS modulates cortical activity in humans is to record evoked potentials during stimulation. To date, several studies focused on motor evoked potentials (MEP) elicited by transcranial magnetic stimulation (TMS) of the primary motor cortex (M1) and found that tACS modulates M1 excitability in a frequency- and time-specific manner (Pozdniakov et al., 2021; Feurra et al., 2011; Guerra et al., 2016; Nowak et al., 2017). In contrast, evidence of tACS effects on cortical evoked responses in the primary somatosensory cortex (S1) are lacking.

* Corresponding author at: Department of Human Neurosciences and IRCCS Neuromed, Sapienza University of Rome, Viale dell'Università 30, Rome 00185, Italy.
E-mail address: alfredo.berardelli@uniroma1.it (A. Berardelli).

https://doi.org/10.1016/j.neuroimage.2022.119119.
Received 28 October 2021; Received in revised form 16 February 2022; Accepted 19 March 2022
Available online 20 March 2022.

In this regard, studies using tACS on S1 have only hypothesized cortical entrainment based on changes in behavioral measures (Gundlach et al., 2016; Neuling et al., 2012; Riecke et al., 2015; Manzo et al., 2020).

In the present study, we tested whether tACS is able to modulate somatosensory information processing at the cortical level, as assessed by recording the N20 and P25 components of the somatosensory-evoked potentials (SEPs). We adopted recently-introduced artifact rejection techniques which allowed to reliably record cortical evoked potentials during tACS (Kohli and Casson, 2019; Helfrich et al., 2014; Neuling et al., 2017; Kasten and Herrmann, 2019; Fehér et al., 2017). In a sham-controlled experimental design, we used a tACS-electroencephalography (EEG) co-registration approach and recorded SEPs during tACS over the primary somatosensory cortex (S1). Several EEG and magnetoencephalography (MEG) studies on human subjects demonstrated that the activity of neuronal populations oscillating at 8–13 Hz over the somatosensory cortex (mu rhythm) can influence early cortical processing of somatosensory stimuli (Zhang and Ding, 2010; Jones et al., 2009; Forschack et al., 2017; Saito et al., 2021). Hence, we used tACS delivered at the specific mu frequency recorded in each subject (individual mu frequency). In addition, tACS was also delivered at the individual beta frequency over S1 since a few observations have suggested a role of beta rhythm in cortical somatosensory functions (Lalo et al., 2007; Baumgarten et al., 2015; Haegens et al., 2011a). To verify whether tACS effects on S1 only occur when the stimulation frequency is resonant to the endogenous rhythms of this area (Ali et al., 2013; Krause et al., 2019; Johnson et al., 2020), we used theta-tACS as a control condition. Indeed, theta rhythm has no major role in somatosensory cortical processing (Cheyne, 2013). To exclude that possible cortical SEPs changes during tACS were due to indirect modifications in subcortical pathways, we also recorded peripheral (N9) and spinal (N13) SEPs components. Furthermore, we recorded early and late components of high-frequency oscillations (HFOs), expressions of thalamocortical and intracortical processing of somatosensory input, and long-latency reflexes (LLRs), which reflect transmission of somatosensory information to the motor cortex. Finally, to clarify whether possible neurophysiological changes were limited to the stimulation period ('online' effects) or persisted beyond the stimulation period, we recorded SEPs before, during, and after mu-tACS in a separate experiment.

Based on the proposed mechanism of action of tACS, we hypothesized that tACS would enhance the processing of somatosensory information through the modulation of resonant neurons when delivered at mu and beta frequencies over S1 (frequency-specific effect). Accordingly, our hypothesis implies that tACS would modulate cortical, but not peripheral or spinal, SEPs components. Also, we hypothesize that tACS effects would be present only 'online' (time-specific effect).

2. Materials and methods

2.1. Participants

Fifteen healthy right-handed (Oldfield, 1971) subjects (mean age ± 1 standard deviation: 30.1 ± 1.6 years; 5 females) were enrolled in the study. The minimal neurophysiologically relevant increase (effect size) was set at 20% change between sham and mu-tACS conditions. This effect was deemed reasonable on the basis of a previous SEPs study (Rocchi et al., 2016), where N20 changed by 26% after theta burst stimulation (from 2.95 ± 0.67 μV at baseline to 2.18 ± 0.59 μV at T1). In order to have a power of 80% of recognizing as statistically significant (at two-sided alpha level 0.05) a real vs. sham N20 change of 0.6 μV, assuming SD=0.7 μV and a within-subjects correlation $r = 0.5$, the minimum required sample was 15 subjects. All subjects were recruited from the Department of Human Neurosciences, Sapienza University of Rome. None of the subjects had psychiatric or neurological disorders or were taking medications acting on the central nervous system at the time of the experiment. None of the participants had contraindications to non-invasive brain stimulation (Rossi et al., 2021). The study was approved by the local ethics committee and conducted in accordance with the Declaration of Helsinki.

2.2. Experimental design

All subjects participated in two separate experiments (experiments 1 and 2), conducted at least 1 week apart and carried out from 10:00 a.m. to 1:00 p.m. Subjects were comfortably seated on a chair designed for EEG recording (EMS, Italy) with their forearms resting on armrests, and were asked to focus on a white cross displayed at the center of a computer screen positioned 70 cm away. The first part of experiment 1 was dedicated to recording individual somatosensory mu and beta frequencies with EEG (see below). Then, subjects underwent SEPs and LLRs recordings during four different stimulation conditions, applied in a randomized order: (1) sham-tACS; (2) mu-tACS; (3) beta-tACS; and (4) theta-tACS. In all conditions, tACS started 20 s before the peripheral electrical stimulation. SEPs and LLRs recordings lasted approximately 7 min overall and were followed by a 20 min pause. In experiment 2, the time course of mu-tACS effects was specifically studied and SEPs were recorded before (T0), during (T1), and 1 min (T2) and 10 min (T3) after stimulation (Fig. 1A).

2.3. tACS

tACS was delivered using a BrainSTIM (EMS, Italy) connected to two rubber 3-cm-diameter round stimulating electrodes attached to the scalp using conductive Ten20 paste (Weaver and Company, USA), ensuring no paste was applied outside the stimulating electrode contact area (Marshall et al., 2016). Using neuronavigation (Softaxic, EMS, Italy), with an optical tracking system (Polaris Vicra, Northern Digital Inc., Canada), we sampled 23 points from the scalp of each participant and adapted the reconstructed brain in the Talairach space using non-linear fitting. The stimulating electrode was positioned over the scalp area corresponding to S1, located using Talairach coordinates ($x = -40$, $y = -30$, $z = 54$) (Boakye et al., 2000), with reference over Pz. Stimulating electrode impedance was kept <10 kΩ. We delivered tACS with a 3-s ramp-up and ramp-down period and no DC offset. Sham-tACS stimulation consisted of ramp-up, 1-s stimulation at the individual mu frequency, and ramp-down. The frequency used for theta-tACS was 6 Hz. Stimulation intensity was titrated from a peak-to-peak amplitude of 1 mA down to the highest intensity that did not induce visual or skin sensations. This procedure resulted in a stimulation intensity of 0.30 ± 0.15 mA for mu-tACS and 0.35 ± 0.17 mA for beta-tACS. Although 1-mA theta-tACS did not induce side effects, we used the mean value between mu- and beta-tACS intensity in each subject for theta-tACS in order to avoid possible intensity-related confounding. Accordingly, theta-tACS stimulation intensity was 0.32 ± 0.14 mA Fig. 1.D shows the current density distribution for mu-tACS in a representative subject with the montage and mean intensity used.

2.4. EEG and electromyography

EEG was recorded from 32 Ag-AgCl electrodes mounted on an elastic cap (EASYCAP, Germany; 10–20 international standard layout). POz and FPz served as a reference and ground, respectively. Channel impedance was kept below 5 kΩ. Electromyography (EMG) was recorded using a pair of surface electrodes placed in a belly-tendon montage over the right abductor pollicis brevis (APB) muscle. EEG and EMG were filtered (DC-3.5 kHz) and sampled at 20 kHz using a TMS-compatible EEG system (NeurOne, Bittium, Finland). EEG data was analyzed using customized scripts on the Matlab platform (R2020a, The Mathworks, USA) and the open source Matlab toolboxes EEGLAB (Delorme and Makeig, 2004), Fieldtrip (Oostenveld et al., 2011), and TESA (Rogasch et al., 2017).

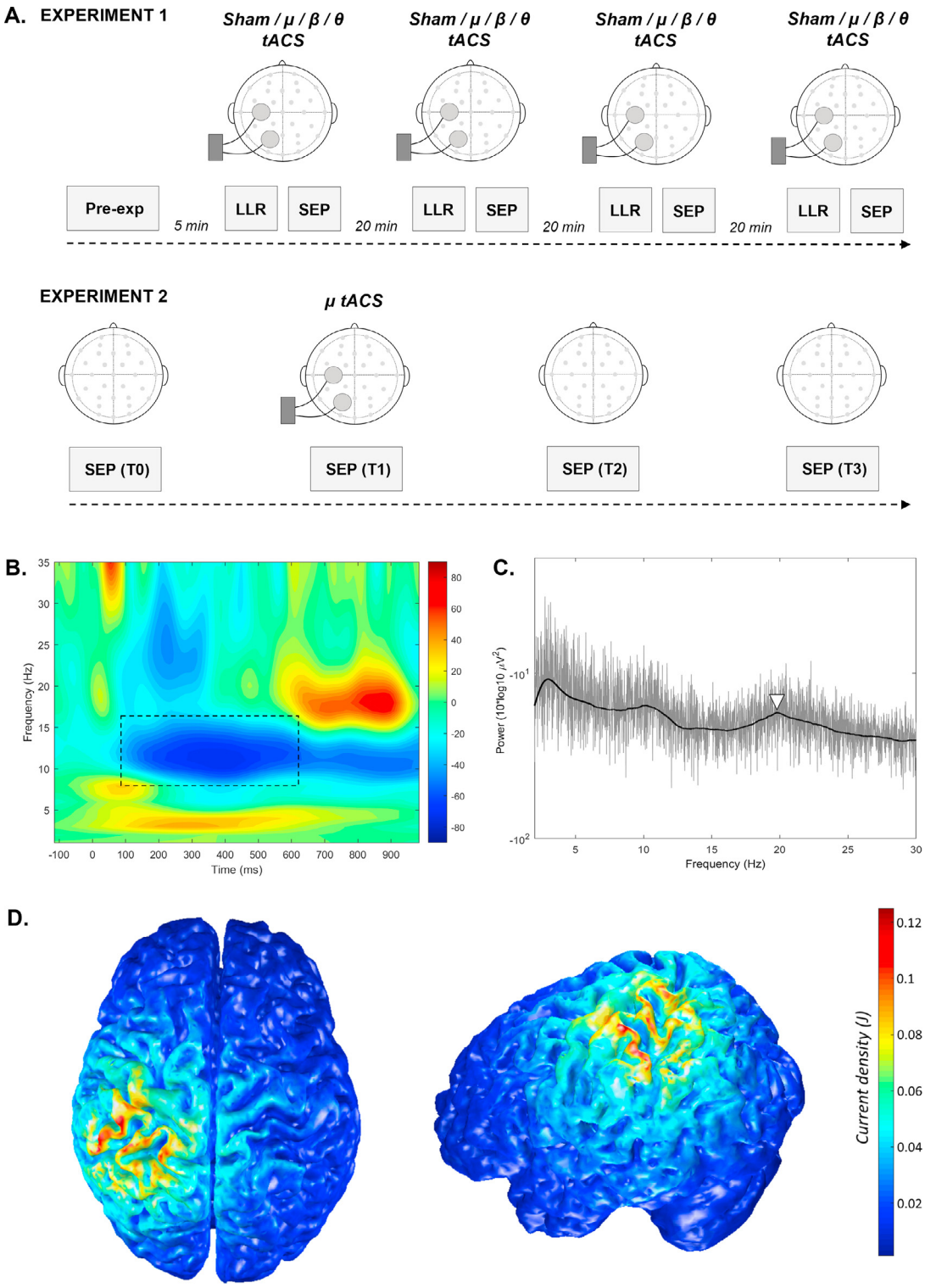

Fig. 1. Experimental design. A. Experiment 1 began with the identification of individual mu (μ) and beta (β) frequency peaks in each subject. Then, subjects underwent SEPs and LLRs recordings during four stimulation conditions applied in a randomized order: (1) sham-tACS; (2) μ-tACS; (3) β-tACS; and 4) theta (θ)-tACS. In experiment 2, the time course of mu-tACS effects was specifically studied and SEPs were recorded before (T0), during (T1), and 1 min (T2) and 10 min (T3) after stimulation (tACS OFF). B. Time-frequency plot from the somatosensory stimulation applied for the mu peak identification in a representative subject. Data were recorded over the CP3 electrode and expressed as percentage change with respect to the average value of a baseline period (−600 to −200 ms). A clear ERD in the mu range (8–13 Hz) was displayed in a time window ranging from 200 to 600 ms (marked in the box). The frequency (1 Hz resolution) in the mu range showing the maximum desynchronization was selected as individual mu frequency for that subject. C. Resting state-EEG spectrogram from a representative subject; the white arrowhead indicates the highest power spectral density value in the beta range used for beta-tACS in that subject. D. Current density distribution of mu-tACS in a representative subject. The MATLAB toolbox Comets2 was used to estimate the current density distribution (http://www.cometstool.com) (Lee et al., 2017) produced with our montage, stimulating electrode size and mean intensity applied for mu-tACS (0.35 mA).

2.5. Individual mu and beta frequency identification

To identify individual mu frequency, subjects underwent a somatosensory stimulation experiment with concurrent EEG recording. One hundred and fifty square-wave electrical pulses (interstimulus interval: 3 s with 50% jitter, ≈7 min in total) were delivered at rest using a constant-current stimulator (Digitimer DS7A) through surface skin electrodes (anode located 0.5 cm distally to the cathode) placed on the distal phalanx of the right index finger. Stimulation was set at the intensity that induced an easily detectable, but not painful, stimulus. EEG data were epoched (−1000 to 1000 ms) around the electrical stimulus and artifacts were manually removed with independent component analysis (ICA) using the FastICA algorithm (Korhonen et al., 2011). Time-frequency power spectra were computed on the epoched EEG data from the CP3 electrode using time-domain complex Morlet wavelet convolution (Bruns, 2004; Cohen, 2019). Wavelet frequency ranged from 2 to 35 Hz with 0.1-Hz increments, and the number of cycles was set to 5 as in previous studies (Gundlach et al., 2016). Percentage change was computed with respect to the average value of a baseline period (−600 to −200 ms) in order to obtain stimulus-related changes in power for each frequency over time. Within the mu (8–13 Hz) band, the frequency with the maximum event-related desynchronization (ERD), i.e., the maximum decrease in power, in a time window ranging from 200 to 600 ms was extracted and used for mu-tACS (Fig. 1B). Somatosensory stimulation also induced desynchronization in the beta frequency range, but this was present in <50% of participants. To detect individual beta frequency, subjects underwent a 5-min resting-state EEG recording. EEG was epoched and cleaned with one round of ICA. Then, cleaned epochs were tapered using a Hanning window, and power spectral density values were computed between 2 and 35 Hz using the fast Fourier transform. The frequency with the highest power spectral density value in the beta range (14–30 Hz) was then detected and used for beta-tACS (Fig. 1C).

2.6. SEPs recording and analysis

Cortical N20 and P25 SEP components were recorded with the active electrode placed at CP3 and the reference electrode at Fz. Peripheral (N9) components were recorded with the active and reference electrode placed over the ipsilateral (Epi) and contralateral (Epc) Erb's point, respectively. Electrodes over the 7th cervical spinous process (Cv7) and over the anterior cervical region (AC) in a Cv7-AC montage were used to record spinal components (N13). The right median nerve was stimulated at the wrist using the Digitimer DS7A, with the anode placed on the wrist crease and the cathode placed 2 cm proximal. Stimuli were monophasic square-wave pulses, with a duration of 200 μs, delivered at 4.4 Hz (1000 traces) and with an intensity set above sensory threshold but just below motor threshold, determined by inspection of the EMG trace recorded from the right APB muscle (Lalo et al., 2007). To extract SEPs, EEG data were first bandpass filtered (1–100 Hz; 4th order Butterworth filter). To remove the large tACS-related electrical stimulation artifact from the EEG recording, we adopted the superimposition of moving average (SMA) approach, which constructs a time-localized template of the artifact and then subtracts it from the collected data (Kohli and Casson, 2019; Kasten and Herrmann, 2019; Kohli and Casson, 2015). Briefly, data from each channel were first epoched in N non-overlapping segments so that the length of each segment matched the period of tACS frequency. Then, each segment and a number (M) of neighboring segments were central moving averaged to create a time-localized artifact template for that segment. The templates of all segments were then concatenated to form an artifact template for each channel, which was then subtracted. Based on previous studies, M was set as 5% of N[46]. EEG data were then epoched (−50 to 150 ms) around the stimulus artifact, cut and interpolated from −5 to 5 ms to remove the artifact arising from peripheral nerve stimulation and avoid stimulus-related ringing artifacts, downsampled (5 kHz) and notch filtered. Residual tACS-related artifacts were captured and manually rejected by running a principal component analysis (PCA) over all 32 channels. PCA resulted in rejection of 1.67 ± 1.05 (mean ± SD) components for mu-tACS, 1.47 ± 0.52 components for beta-tACS, and 1.27 ± 0.46 components for theta-tACS. Eye blinks, movements, and muscle-related and other identified artifacts were captured and manually rejected with one round of ICA. Finally, after re-referencing data to Fz, N20 and P25 peak latencies and N20 and P25 absolute amplitude (measured from the DC-removed zero baseline) were calculated in all subjects from the CP3-Fz channel (see Supplementary Fig. 1 for SEP analysis steps in one representative subject). EEG data analysis from the sham-tACS recording followed identical preprocessing steps, except for SMA and PCA, which were not performed.

2.7. HFO analysis

To extract HFOs from the underlying N20, raw EEG data were first bandpass filtered (1–800 Hz; 4th order Butterworth filter) and then underwent tACS artifact removal using SMA. Data were then epoched (−50 to 150 ms) around the stimulus artifact, cut and interpolated from −5 to 5 ms to avoid stimulus-related ringing artifacts, bandpass filtered (450–750 Hz; 4th order Butterworth filter) and downsampled (5 kHz). To remove residual tACS-related artifacts PCA was run, and resulted in rejection of 2.36 ± 1.28 components for mu-tACS, 2.53 ± 1.36 components for beta-tACS, and 1.87 ± 0.83 components for theta-tACS. In the final averaged data, two burst components in the HFO waveform separated by the N20 peak, early (e-HFO) and late (l-HFO), were identified. The beginning of the e-HFO was identified with reference to the onset latency of the N20 component on the corresponding SEP trace, whereas the end of the L-HFO burst was defined by the last wave that had a 50% larger amplitude (measured peak-to-trough) than the average noise calculated in the interval from 35 to 40 ms after the electrical stimulus, as described in previous studies (Restuccia and Coppola, 2015) (see Supplementary Fig. 2 for time-domain and power spectra of HFOs during sham- and mu-tACS in one representative subject). Burst amplitudes for e-HFO and L-HFO waves were measured as the area under the rectified waveform (area under the curve, AUC).

2.8. LLR recording and analysis

Electrical stimuli (200-μs-duration square-wave pulses; 3 Hz repetition rate) were delivered over the right median nerve at motor threshold and EMG responses were recorded over the APB muscle. Electrical stimuli were delivered while subjects maintained a stable contraction leaning the thumb against the little finger. Since only LLR II was present in all subjects, LLR II peak-to-peak amplitude was measured according to standardized procedures (Deuschl et al., 1988; Cruccu and Deuschl, 2000).

2.9. Statistical analysis

To compare the stimulation intensity used for mu-, beta-, and theta-tACS, we used a repeated measures (RM)-ANOVA with the factor "stimulation" (3 levels: mu-tACS, beta-tACS, theta-tACS). Separate RM-ANOVAs with the factor "frequency" (4 levels: sham-tACS, mu-tACS, beta-tACS, theta-tACS) and "wave" (2 levels: N20, P25) were applied to assess the effects of tACS on the latency and amplitude of cortical SEPs components (experiment 1). Two additional RM-ANOVAs with "frequency" and "wave" as factors were tested to verify the effects of tACS on peripheral/spinal SEPs components (2 levels: N9, N13) and HFOs (2 levels: e-HFO, L-HFO). In case of a significant "frequency" x "wave" interaction, separate follow-up RM-ANOVAs with "frequency" as main factor of the analysis were applied for each wave. Finally, a RM-ANOVA with the factor "frequency" was also adopted to assess tACS effects on LLRs. The effects detected in the various RM-ANOVAs were further analyzed using Bayesian statistics (Rouder et al., 2009). RM-ANOVA Bayesian equivalent for each neurophysiological measure was computed and, only for those with a Bayes Factor smaller than 1/3 (Null

versus Alternative hypothesis), Bayes equivalent paired t-tests were performed. As priors, we used uninformative priors and specifically diffuse (uniform). For sensitivity analysis, we used also one of the Jeffrey's rules for non-informative (prior $\propto 1/\sigma 20$). To assess mu-tACS-related changes in SEPs parameters over time (experiment 2), we used an RM-ANOVA with "time" as a factor (4 levels: T0, T1, T2, and T3). Greenhouse-Geisser corrections were applied when a violation of sphericity in Mauchly's tests was detected. T-test was used for post-hoc comparisons and Bonferroni's correction was applied for multiple comparisons. Finally, we compared the amount of N20 modulation during mu-tACS in experiments 1 and 2 using a paired *t*-test. Then, we verified the possible correlation between N20 values during mu-tACS in experiments 1 and 2 using Pearson's correlation test. Statistical analyzes were performed using SPSS Statistics (version 27; IBM). The level of significance was set at $p < 0.05$.

3. Results

The average mu frequency ERD peak was 11.7 ± 1.3 Hz. The average beta frequency peak was 22.6 ± 3.0 Hz (mu and beta frequency peaks for each participant are shown in Supplementary Fig. 3). The stimulation intensity used for mu-tACS, beta-tACS, and theta-tACS did not differ, as revealed by the non-significant factor "stimulation intensity" in the RM-ANOVA ($F_{2,28} = 1.49$, $p = 0.24$).

3.1. Experiment 1: frequency-dependent tACS effects

tACS differentially influenced the various cortical SEPs components, as indicated by the significant "frequency" x "wave" interaction in the RM-ANOVA ($F_{3,42} = 4.31$, $p = 0.01$, $\eta_p^2 = 0.24$, observed power = 0.83). In particular, the N20 absolute amplitude was modulated by tACS, as demonstrated by the significant factor "frequency" in the follow-up RM-ANOVA ($F_{3,42} = 5.56$, $p < 0.01$, $\eta_p^2 = 0.28$, observed power = 0.92). Post-hoc analysis revealed greater N20 amplitude during mu-tACS compared to both sham-tACS ($p < 0.01$) and theta-tACS ($p = 0.02$) (Fig. 2). No differences were observed between N20 amplitude during sham-tACS, beta-tACS (sham-tACS vs beta-tACS: $p = 0.33$) and theta-tACS (sham-tACS vs theta-tACS: $p = 0.99$). In contrast, the P25 amplitude ($F_{3,42} = 0.25$, $p = 0.86$, $\eta_p^2 = 0.02$) and the latency of N20 and P25 ("frequency": $F_{3,42} = 0.89$, $p = 0.45$, $\eta_p^2 = 0.06$; "frequency" x "wave": $F_{3,42} = 2.29$, $p = 0.13$, $\eta_p^2 = 0.14$) were similar between the four stimulation conditions (Fig. 2). Analysis of peripheral SEP components revealed no differences between tACS conditions in N9 and N13 amplitude ("frequency": $F_{3,42} = 1.18$, $p = 0.33$, $\eta_p^2 = 0.09$; "frequency" x "wave": $F_{3,42} = 0.93$, $p = 0.43$, $\eta_p^2 = 0.07$). Similarly, tACS did not change the e-HFO and L-HFO AUC ("frequency": $F_{3,42}$=0.14, $p = 0.86$, η_p^2=0.01; "frequency" x "wave": $F_{3,42} = 0.74$, $p = 0.45$, $\eta_p^2 = 0.05$), or LLRs amplitude, as demonstrated by the non-significant factor "frequency" in the RM-ANOVA (LLR: $F_{3,42} = 1.24$, $p = 0.31$, $\eta_p^2 = 0.07$)(Fig. 3). The non-significant difference in N9, N13, P25, e-HFO, L-HFO and LLRs between conditions was also supported by Bayesian statistics, showing moderate to extreme evidence in favor of the null hypothesis. Bayesian analysis on N20 instead demonstrated strong evidence in favor of the alternative hypothesis (Supplementary Table 1). In conclusion, cortical processing of somatosensory information, as measured with N20 amplitude, was facilitated by tACS delivered at individual mu frequency, whereas P25 amplitude, peripheral SEP components, e-HFO, L-HFO, and LLRs did not change.

3.2. Experiment 2: time-dependent tACS effects

The analysis demonstrated that N20 amplitude changed over time, as suggested by the significant factor "time" ($F_{3,42} = 6.93$, $p < 0.001$, $\eta_p^2 = 0.33$, observed power = 0.97). Post-hoc analysis revealed that N20 amplitude selectively increased during mu-tACS (T1) compared to baseline (T0) ($p < 0.01$), T2 ($p = 0.02$), and T3 ($p = 0.001$). Notably, N20 amplitude was similar between T0, T2, and T3 ($p > 0.05$) (Fig. 4). When we compared N20 amplitude during mu-tACS in experiments 1 and 2, the analysis revealed similar values between the two different experimental sessions ($t = 0.69$, $p = 0.50$). Furthermore, N20 amplitude during mu-tACS in experiments 1 and 2 was positively correlated ($r = 0.52$, $p = 0.04$). Overall, these results suggest that mu-tACS effects are limited to the stimulation period and are reliable.

4. Discussion

In the present study, we demonstrated that tACS delivered at mu frequency over S1 increased N20 amplitude, while beta-, theta-, and sham-tACS had no effect. N20 latency, P25 amplitude and latency, and the amplitude of peripheral (N9) and spinal (N13) SEP components did not change during tACS. Moreover, mu-, beta-, and theta-tACS did not modulate the e-HFO or L-HFO AUC or LLRs amplitude. We also showed that N20 amplitude increased only during stimulation, i.e., it was similar before and after mu-tACS. Overall, these data provide direct evidence that tACS modulates the early processing of somatosensory information at the cortical level in humans, and its effects have frequency- and time-dependent specificity.

One strength of the study is that mu-tACS effects on N20 amplitude demonstrated a good reliability. Indeed, the same subjects participated in experiments 1 and 2, and in both sessions we found a significant N20 amplitude increase during stimulation. Moreover, the amount of facilitation did not differ between sessions, and there was a positive correlation between mu-tACS effects in experiments 1 and 2. We also made sure to control for several factors which could have influenced our results. Mu-, beta-, and theta-tACS intensity did not differ and was carefully titrated in each participant below the threshold that induced skin or visual sensations. This procedure allowed to avoid any possible influence of tACS-related somatosensory side effects on SEPs amplitude modulation and ensured that participants were unable to distinguish between real and sham stimulation, thus resulting in a proper blinding procedure. The four tACS stimulation conditions were applied in randomized order and we waited 20 min between stimulation conditions to avoid possible carryover effects. Previous studies have found that residual tACS-related artifacts surviving the data analysis algorithms may contaminate EEG recordings at stimulation frequencies, their harmonics, and side-bands (Kasten and Herrmann, 2019; Noury et al., 2016; Noury and Siegel, 2017a, 2017b). While we cannot fully exclude that minimal residual artifacts survived our SMA, PCA, and ICA procedures, we believe it is unlikely that they influenced our results. Indeed, recent studies showed that the template subtraction approach ensures reliable cortical evoked-potentials waveform reconstruction and measurement, even if tACS-related artifacts are present (Kohli and Casson, 2019; Helfrich et al., 2014; Fehér et al., 2017). Furthermore, even if case residual artifacts survived our preprocessing methodology, they would have similarly contaminated EEG recordings during mu-, beta-, and theta-tACS, thus not justifying the specific N20 amplitude modulation we observed with mu-tACS.

The main finding of our study was that tACS applied at individual mu frequency, but not at individual beta or theta frequency, enhanced the amplitude of the N20 SEP component recorded over the contralateral somatosensory cortex. The effect of tACS in modifying the spike timing of neuronal populations is known to be frequency dependent and strictly related to the so-called 'endogenous resonance principle'. That is, tACS effects are prominent when the stimulation frequency matches or is very close to the endogenous rhythm of the targeted cortical site (Ali et al., 2013; Antal and Paulus, 2013). Accordingly, the frequency specificity of tACS effects we observed points to a prominent role of S1 mu oscillations in influencing the processing of somatosensory information. This finding is fully in line with the literature linking mu oscillations to information processing in somatosensory brain regions (Pineda, 2005), and in particular to the results of previous MEG and EEG studies conducted in healthy humans showing an association between high pre-stimulus

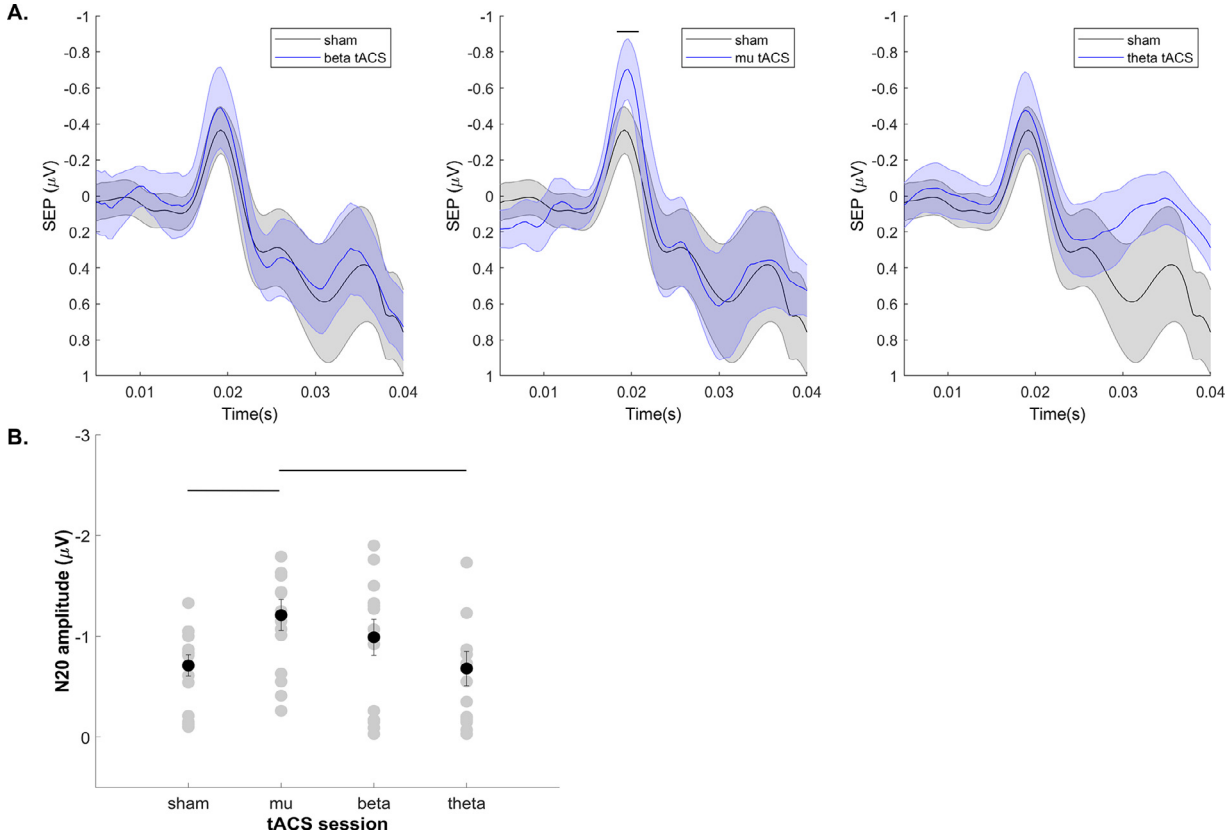

Fig. 2. Frequency-dependent effects of tACS on N20. A. Grand-average plot displaying mean and standard error of SEP N20 component during beta-, mu- and theta-tACS compared to sham-tACS. B. Single-subject (gray dots) and group mean (black dot) and standard error of the mean (bars) values of N20 in each stimulation condition. The N20 amplitude was greater during mu-tACS compared to both sham-tACS and theta-tACS. No differences were observed between N20 amplitude during sham-tACS, beta-tACS, and theta-tACS. The horizontal bars represent significant post-hoc comparisons.

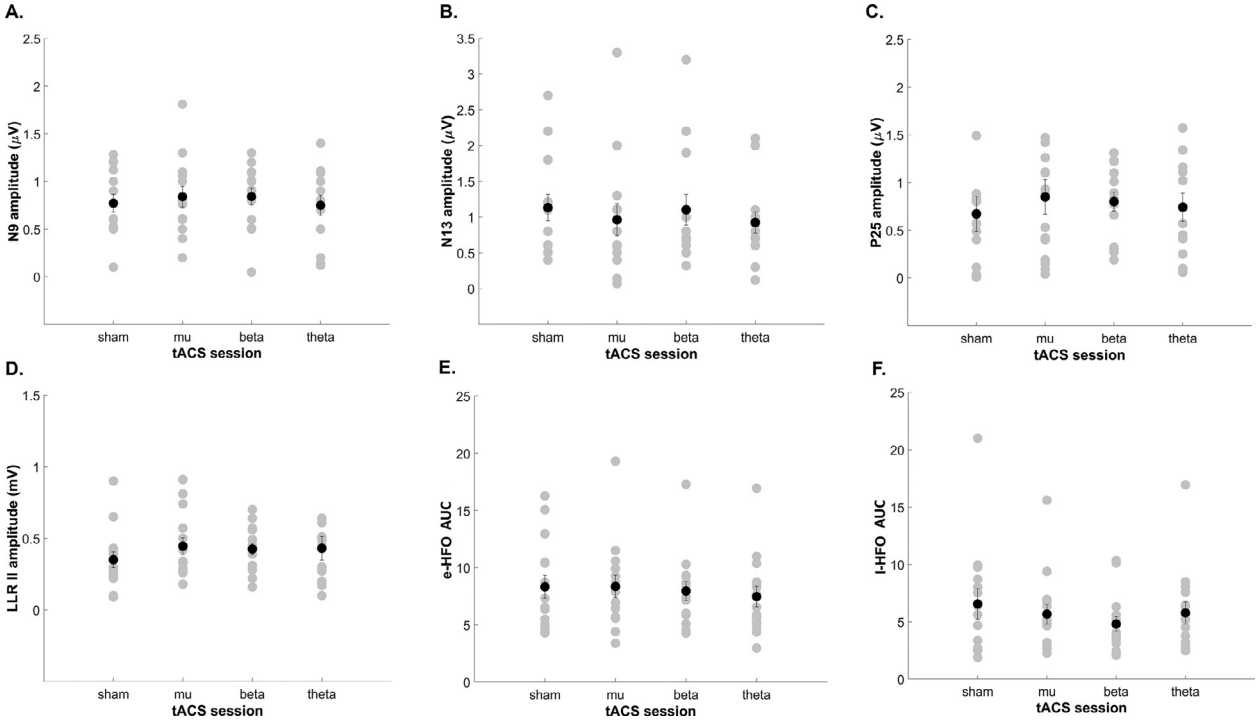

Fig. 3. Effects of tACS on peripheral and spinal SEP components, P25, LLRs and HFOs. Single-subject (gray dots) and group mean (black dot) and standard error of the mean (bars) values of N9 (A), N13 (B), P25 (C), LLR II (D), e-HFO (E) and L-HFO (F) during sham-, mu-, beta-, and theta-tACS. The N9, N13 and P25 amplitude was similar between the four tACS conditions. Similarly, tACS did not change LLRs amplitudes and e-HFO or L-HFO AUC.

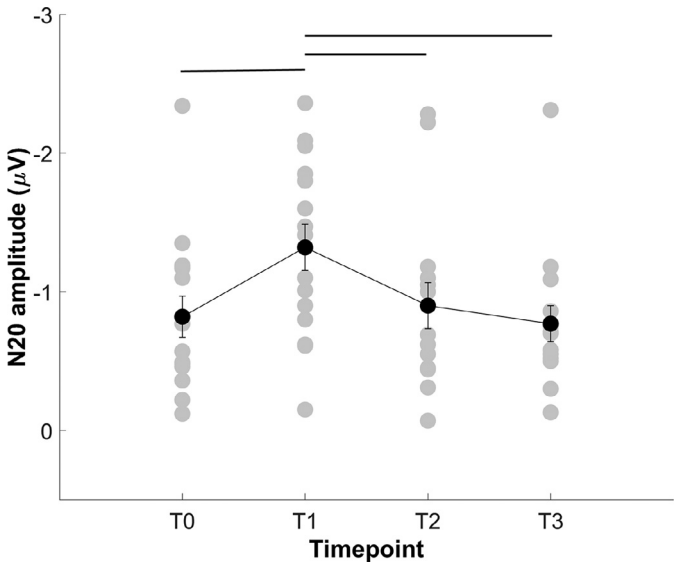

Fig. 4. Time-dependent effects of mu-tACS. SEPs were recorded before (T0), during (T1), and 1 min (T2) and 10 min (T3) after tACS applied at the individual mu frequency. The N20 amplitude increased during mu-tACS (T1) compared to baseline (T0), T2, and T3. No differences were observed between the N20 amplitude at T0, T2, and T3. The black dots and bars represent mean values and standard error of the mean, respectively. Individual subjects' data are displayed in gray. The horizontal bars represent significant differences at post-hoc comparisons.

mu power over S1 and enhanced early somatosensory-evoked responses over S1 (Zhang and Ding, 2010; Jones et al., 2009; Nikouline et al., 2000; Ziegler et al., 2010). In addition, invasive recordings in animals revealed increased spike-firing rates in S1 during periods with high alpha power (Haegens et al., 2011b).

The evaluation of all SEP components and the assessment of HFOs and LLRs during stimulation allowed us to clarify the neuronal circuit possibly responsible for the N20 amplitude increase induced by mu-tACS. Previous studies have demonstrated that activation of sensorimotor cortical areas can gate the transmission of afferent sensory information at various subcortical levels (Insola et al., 2004; Rossini et al., 1999; Wasaka et al., 2003; Lei et al., 2018). However, in our study, tACS applied at individual mu frequency did not change subcortical N9 and N13 SEP components, which are generated in the brachial plexus and cervical dorsal horn gray matter, respectively. Hence, we can exclude the possible influence of peripheral or spinal structures on mu-tACS effects on N20.

Moreover, our data showed that mu-tACS does not modulate HFO amplitude. Previous evidence demonstrated that e-HFO reflect the action potentials of thalamocortical fibers projecting to area 3b of the somatosensory cortex, while L-HFO represent the activity of layer IV fast-spiking GABA-ergic inhibitory interneurons connected to pyramidal neurons receiving thalamocortical fibers (Ozaki and Hashimoto, 2011). Since mu-tACS failed to modify both e-HFO and L-HFO we could also exclude the possibility that N20 amplitude increase was secondary to changes in thalamocortical output or layer IV GABA-ergic interneuron activity. Similarly, mu-tACS also did not change LLRs amplitude, a measure reflecting the activity of intracortical somatosensory relay neurons responsible for transmission of peripheral afferent stimuli to the primary motor cortex (Bawa et al., 1979; Evarts and Fromm, 1981). Hence, we can exclude that N20 modulation during mu-tACS depends on modifications in afferent pathways within the dorsal column/medial lemniscal system to the sensorimotor cortex.

We therefore suggest that mu-tACS directly acts on S1 and possibly on neurons located in superficial cortical layers. Indeed, data from invasive recordings in animals show that frequency-specific tACS effects are limited to the more superficial layers of the stimulated cortex (Ali et al., 2013). Furthermore, a recent electrocorticography study in epilepsy patients demonstrated that mu rhythm is primarily generated by layer I-III neurons (Halgren et al., 2019). The N20 wave is thought to derive from excitatory postsynaptic potentials of layer IV pyramidal neurons leading to a superficially-directed current in Brodmann's area 3b (Allison et al., 1991; Valeriani and Le Pera, 2006). Accordingly, we hypothesize that mu-tACS entrains mu-resonant neurons in superficial S1 layers, which in turn leads to the facilitation of pyramidal neurons responsible for N20 generation. Both the reduction in interneuronal inhibition and the increase in excitation may determine pyramidal neuron facilitation. Despite the difficulty in establishing the precise mechanism underlying mu-tACS effects, we found that mu-tACS did not affect the P25 wave, which reflects GABA-ergic neurotransmission in S1 (Valeriani et al., 1998; Restuccia et al., 2002). Thus, we favor increased excitation as the possible neurophysiological substrate of mu-tACS effects on early S1 processing of sensory input.

Another relevant study finding concerns the timing of mu-tACS effects on N20 amplitude. In experiment 2, we found that N20 amplitude significantly increased during stimulation (T1) and this effect was not present at T2 or T3. These data clearly indicate that mu-tACS effects were limited to the stimulation time ("online"). The entrainment effect produced by tACS reflects the temporal alignment of endogenous rhythmical brain activity with exogenous alternating currents (Thut et al., 2011). In line with this mechanism, current evidence demonstrates that neurophysiological tACS effects reflecting entrainment take place only "online", i.e., during stimulation (Guerra et al., 2019, 2020; Bologna et al., 2019; Pozdniakov et al., 2021; Vossen et al., 2015). In contrast, tACS aftereffects, as shown in studies delivering ripple frequency stimulations, are thought to be driven by synaptic plasticity mechanisms rather than outlasting entrainment "echoes" (Guerra et al., 2020; Moliadze et al., 2021). Accordingly, the lack of N20 modulation we observed after stimulation further indicates that mu-tACS effects do not reflect plasticity mechanisms, but likely derive from successful entrainment of cortical neurons.

Finally, we found comparable N20 amplitude between beta- and sham-tACS conditions, possibly suggesting that beta rhythm does not significantly influence cortical somatosensory processing. This result apparently contrasts with a previous EEG study showing enhanced N20 during beta activity increase (Lalo et al., 2007). However, motor cortex (fronto-central channels) beta power, and sensorimotor beta coherence were measured in that study (Lalo et al., 2007), whereas we focused tACS current on the post-central gyrus, as demonstrated by our modeling data. Thus, we believe that it is unlikely that beta-tACS modulated motor cortex beta or sensorimotor beta coherence. The lack of N20 modulation during beta-tACS may also be due to neuroanatomical reasons. Beta oscillations are thought to originate from deeper cortical layers (Sherman et al., 2016) than the mu rhythm (Halgren et al., 2019), and tACS may produce stronger effects on superficial layer neurons. Finally, because there is a direct relationship between the stimulation intensity required to entrain neurons and the frequency targeted (Reato et al., 2013), it is possible that the intensity we adopted was sufficient for successful entrainment of somatosensory mu (8–13 Hz), but not beta (13–30 Hz) resonant neurons.

We acknowledge the use of relatively low tACS intensities as a limitation of our study. However, we used these intensities in order to avoid possible skin sensations and achieve a properly blinded study. To soften this limit, we used a small stimulating electrode size, which results in higher current density over the scalp than that produced by common 5 × 7-cm stimulating electrodes. In addition, we applied tACS at individual, i.e., endogenous, frequencies, and lower stimulation intensities may suffice to modulate superficially-located cortical neurons (Ali et al., 2013; Krause et al., 2019; Frohlich and McCormick, 2010; Schmidt et al., 2014). However, we cannot fully exclude that SEP components could be modulated by tACS delivered at frequency bands other than mu (e.g., beta) using high stimulation intensities. Finally, although our findings

are in line with the mechanisms underlying entrainment (i.e. frequency- and time-specificity), we did not directly measure entrainment in our EEG data.

5. Conclusion

In conclusion, we demonstrated that tACS applied at individual mu frequency over S1 is able to modulate early processing of somatosensory information at the cortical level, as measured with SEP N20 amplitude, and that the effect is strictly limited to the stimulation period. Together with a few previous observations (Helfrich et al., 2014; Helfrich et al., 2016; Herring et al., 2019), this result represents a direct demonstration of tACS effects on cortical neuronal activity in humans, and likely reflects successful entrainment of resonant neuronal populations. Successful modulation of S1 activity by tACS may lead to applications in neurological disorders characterized by altered somatosensory function.

Declarations of Competing Interest

None.

Credit authorship contribution statement

Andrea Fabbrini: Conceptualization, Methodology, Software, Writing – original draft, Writing – review & editing. **Andrea Guerra:** Methodology, Formal analysis, Writing – original draft, Writing – review & editing. **Margherita Giangrosso:** Investigation, Formal analysis, Writing – original draft. **Nicoletta Manzo:** Investigation, Visualization. **Giorgio Leodori:** Writing – review & editing, Supervision. **Patrizio Pasqualetti:** Writing – review & editing, Formal analysis. **Antonella Conte:** Writing – review & editing, Supervision. **Vincenzo Di Lazzaro:** Writing – review & editing, Supervision. **Alfredo Berardelli:** Writing – review & editing, Supervision.

Acknowledgments

None.

Funding

This research did not receive any specific grant from funding agencies in the public, commercial, or non-for-profit sectors.

Data availability statement

Data from our study are available from the corresponding author upon reasonable request.

Supplementary materials

Supplementary material associated with this article can be found, in the online version, at doi:10.1016/j.neuroimage.2022.119119.

References

Ali, M.M., Sellers, K.K., Fröhlich, F., 2013. Transcranial alternating current stimulation modulates large-scale cortical network activity by network resonance. J. Neurosci. Off. J. Soc. Neurosci. 33, 11262–11275.

Allison, T., Wood, C.C., McCarthy, G., Spencer, D.D., 1991. Cortical somatosensory evoked potentials. II. Effects of excision of somatosensory or motor cortex in humans and monkeys. J. Neurophysiol. 66, 64–82.

Antal, A., Paulus, W., 2013. Transcranial alternating current stimulation (tACS). Front. Hum. Neurosci. 7, 317.

Baumgarten, T.J., Schnitzler, A., Lange, J., 2015. Beta oscillations define discrete perceptual cycles in the somatosensory domain. Proc. Natl. Acad. Sci. U. S. A. 112, 12187–12192.

Bawa, P., Stein, R.B., Tatton, W.G., 1979. Dynamics of a long-latency reflex pathway in the monkey. Biol. Cybern. 34, 107–110.

Boakye, M., Huckins, S.C., Szeverenyi, N.M., Taskey, B.I., Hodge, C.J., 2000. Functional magnetic resonance imaging of somatosensory cortex activity produced by electrical stimulation of the median nerve or tactile stimulation of the index finger. J. Neurosurg. 93, 774–783.

Bologna, M., Guerra, A., Paparella, G., Colella, D., Borrelli, A., Suppa, A., Lazzaro, V.D., Brown, P., Berardelli, A., 2019. Transcranial alternating current stimulation has frequency-dependent effects on motor learning in healthy humans. Neuroscience 411, 130–139.

Bruns, A., 2004. Fourier-, Hilbert- and wavelet-based signal analysis: are they really different approaches? J. Neurosci. Methods 137, 321–332.

Cheyne, D.O., 2013. MEG studies of sensorimotor rhythms: a review. Exp. Neurol. 245, 27–39.

Cohen, M.X., 2019. A better way to define and describe Morlet wavelets for time-frequency analysis. Neuroimage 199, 81–86.

Cruccu, G., Deuschl, G., 2000. The clinical use of brainstem reflexes and hand–muscle reflex. Clin. Neurophysiol. Off. J. Int. Fed. Clin. Neurophysiol. 111, 371–387.

Delorme, A., Makeig, S., 2004. EEGLAB: an open source toolbox for analysis of single-trial EEG dynamics including independent component analysis. J. Neurosci. Methods 134, 9–21.

Deuschl, G., Strahl, K., Schenck, E., Lücking, C.H., 1988. The diagnostic significance of long-latency reflexes in multiple sclerosis. Electroencephalogr. Clin. Neurophysiol. 70, 56–61.

Evarts, E.V., Fromm, C., 1981. Transcortical reflexes and servo control of movement. Can. J. Physiol. Pharmacol. 59, 757–775.

Fehér, K.D., Nakataki, M., Morishima, Y., 2017. Phase-dependent modulation of signal transmission in cortical networks through tACS-induced neural oscillations. Front. Hum. Neurosci. 11, 471.

Feurra, M., Bianco, G., Santarnecchi, E., Del Testa, M., Rossi, A., Rossi, S., 2011. Frequency-dependent tuning of the human motor system induced by transcranial oscillatory potentials. J. Neurosci. Off. J. Soc. Neurosci. 31, 12165–12170.

Forschack, N., Nierhaus, T., Müller, M.M., Villringer, A., 2017. Alpha-band brain oscillations shape the processing of perceptible as well as imperceptible somatosensory stimuli during selective attention. J. Neurosci. Off. J. Soc. Neurosci. 37, 6983–6994.

Frohlich, F., McCormick, D, 2010. Endogenous electric fields may guide neocortical network activity. Neuron 67, 129–143.

Giovanni, A., Capone, F., di Biase, L., Ferreri, F., Florio, L., Guerra, A., Marano, M., Paolucci, M., Ranieri, F., Salomone, G., et al., 2017. Oscillatory activities in neurological disorders of elderly: biomarkers to target for neuromodulation. Front. Aging Neurosci 9, 189.

Guerra, A., Pogosyan, A., Nowak, M., Tan, H., Ferreri, F., Di Lazzaro, V., Brown, P., 2016. Phase dependency of the human primary motor cortex and cholinergic inhibition cancelation during beta tACS. Cereb. Cortex 26, 3977–3990 N. Y. NY.

Guerra, A., Suppa, A., Asci, F., De Marco, G., D'Onofrio, V., Bologna, M., Di Lazzaro, V., Berardelli, A, 2019. LTD-like plasticity of the human primary motor cortex can be reversed by γ-tACS. Brain Stimul. 12, 1490–1499.

Guerra, A., Ranieri, F., Falato, E., Musumeci, G., Di Santo, A., Asci, F., Di Pino, G., Suppa, A., Berardelli, A., Di Lazzaro, V., 2020. Detecting cortical circuits resonant to high-frequency oscillations in the human primary motor cortex: a TMS-tACS study. Sci. Rep. 10, 7695.

Gundlach, C., Müller, M.M., Nierhaus, T., Villringer, A., Sehm, B., 2016. Phasic modulation of human somatosensory perception by transcranially applied oscillating currents. Brain Stimul. 9, 712–719.

Haegens, S., Nácher, V., Hernández, A., Luna, R., Jensen, O., Romo, R., 2011a. Beta oscillations in the monkey sensorimotor network reflect somatosensory decision making. Proc. Natl. Acad. Sci. 108, 10708–10713.

Haegens, S., Nacher, V., Luna, R., Romo, R., Jensen, O., 2011b. Oscillations in the monkey sensorimotor network influence discrimination performance by rhythmical inhibition of neuronal spiking. Proc. Natl. Acad. Sci. 108, 19377–19382.

Halgren, M., Ulbert, I., Bastuji, H., Fabó, D., Erőss, L., Rey, M., Devinsky, O., Doyle, W.K., Mak-McCully, R., Halgren, E., et al., 2019. The generation and propagation of the human alpha rhythm. Proc. Natl. Acad. Sci 116, 23772–23782.

Helfrich, R.F., Schneider, T.R., Rach, S., Trautmann-Lengsfeld, S.A., Engel, A.K., Herrmann, C.S., 2014. Entrainment of brain oscillations by transcranial alternating current stimulation. Curr. Biol. 24, 333–339 CB.

Helfrich, R.F., Herrmann, C.S., Engel, A.K., Schneider, T.R., 2016. Different coupling modes mediate cortical cross-frequency interactions. Neuroimage 140, 76–82.

Herring, J.D., Esterer, S., Marshall, T.R., Jensen, O., Bergmann, T.O., 2019. Low-frequency alternating current stimulation rhythmically suppresses gamma-band oscillations and impairs perceptual performance. Neuroimage 184, 440–449.

Herrmann, C.S., Rach, S., Neuling, T., Strüber, D, 2013. Transcranial alternating current stimulation: a review of the underlying mechanisms and modulation of cognitive processes. Front. Hum. Neurosci. 7, 279.

Insola, A., Le Pera, D., Restuccia, D., Mazzone, P., Valeriani, M., 2004. Reduction in amplitude of the subcortical low- and high-frequency somatosensory evoked potentials during voluntary movement: an intracerebral recording study. Clin. Neurophysiol. 115, 104–111.

Johnson, L., Alekseichuk, I., Krieg, J., Doyle, A., Yu, Y., Vitek, J., Johnson, M., Opitz, A., 2020. Dose-dependent effects of transcranial alternating current stimulation on spike timing in awake nonhuman primates. Sci. Adv. 6, eaaz2747.

Jones, S.R., Pritchett, D.L., Sikora, M.A., Stufflebeam, S.M., Hämäläinen, M., Moore, C.I., 2009. Quantitative analysis and biophysically realistic neural modeling of the MEG mu rhythm: rhythmogenesis and modulation of sensory-evoked responses. J. Neurophysiol. 102, 3554–3572.

Kasten, F.H., Herrmann, C.S., 2019. Recovering brain dynamics during concurrent tACS-M/EEG: an overview of analysis approaches and their methodological and interpretational pitfalls. Brain Topogr. 32, 1013–1019.
Kohli, S., Casson, A.J., 2015. Removal of transcranial A.C. current Stimulation artifact from simultaneous EEG recordings by superposition of moving averages. Annu. Int. Conf. IEEE Eng. Med. Biol. Soc. 2015, 3436–3439 IEEE Eng. Med. Biol. Soc. Annu. Int. Conf..
Kohli, S., Casson, A.J., 2019. Removal of gross artifacts of transcranial alternating current stimulation in simultaneous EEG monitoring. Sensors 19, 190.
Korhonen, R.J., Hernandez-Pavon, J.C., Metsomaa, J., Mäki, H., Ilmoniemi, R.J., Sarvas, J., 2011. Removal of large muscle artifacts from transcranial magnetic stimulation-evoked EEG by independent component analysis. Med. Biol. Eng. Comput. 49, 397–407.
Krause, M.R., Vieira, P.G., Csorba, B.A., Pilly, P.K., Pack, C.C., 2019. Transcranial alternating current stimulation entrains single-neuron activity in the primate brain. Proc. Natl. Acad. Sci 116, 5747–5755.
Lalo, E., Gilbertson, T., Doyle, L., Di Lazzaro, V., Cioni, B., Brown, P., 2007. Phasic increases in cortical beta activity are associated with alterations in sensory processing in the human. Exp. Brain Res. 177, 137–145.
Lee, C., Jung, Y.J., Lee, S.J., Im, C.H., 2017. COMETS2: an advanced MATLAB toolbox for the numerical analysis of electric fields generated by transcranial direct current stimulation. J. Neurosci. Methods 277, 56–62.
Lei, Y., Ozdemir, R.A., Perez, M.A., 2018. Gating of sensory input at subcortical and cortical levels during grasping in humans. J. Neurosci. 38, 7237–7247.
Manzo, N., Guerra, A., Giangrosso, M., Belvisi, D., Leodori, G., Berardelli, A., Conte, A., 2020. Investigating the effects of transcranial alternating current stimulation on primary somatosensory cortex. Sci. Rep. 10, 17129.
Marshall, T.R., Esterer, S., Herring, J.D., Bergmann, T.O., Jensen, O., 2016. On the relationship between cortical excitability and visual oscillatory responses - a concurrent tDCS-MEG study. Neuroimage 140, 41–49.
Moliadze, V., Stenner, T., Matern, S., Siniatchkin, M., Nees, F., Hartwigsen, G., 2021. Online effects of beta-tACS over the left prefrontal cortex on phonological decisions. Neuroscience 463, 264–271.
Neuling, T., Wagner, S., Wolters, C.H., Zaehle, T., Herrmann, C.S., 2012. Finite-element model predicts current density distribution for clinical applications of tDCS and tACS. Front. Psychiatry 3, 83.
Neuling, T., Ruhnau, P., Weisz, N., Herrmann, C.S., Demarchi, G., 2017. Faith and oscillations recovered: on analyzing EEG/MEG signals during tACS. Neuroimage 147, 960–963.
Nikouline, V.V., Wikström, H., Linkenkaer-Hansen, K., Kesäniemi, M., Ilmoniemi, R.J., Huttunen, J., 2000. Somatosensory evoked magnetic fields: relation to pre-stimulus mu rhythm. Clin. Neurophysiol. 111, 1227–1233.
Noury, N., Siegel, M., 2017a. Analyzing EEG and MEG signals recorded during tES, a reply. Neuroimage 167, 53–61.
Noury, N., Siegel, M., 2017b. Phase properties of transcranial electrical stimulation artifacts in electrophysiological recordings. Neuroimage 158, 406–416.
Noury, N., Hipp, J.F., Siegel, M., 2016. Physiological processes non-linearly affect electrophysiological recordings during transcranial electric stimulation. Neuroimage 140, 99–109.
Nowak, M., Hinson, E., van Ede, F., Pogosyan, A., Guerra, A., Quinn, A., Brown, P., Stagg, C.J., 2017. Driving human motor cortical oscillations leads to behaviorally relevant changes in local GABAA inhibition: a tACS-TMS study. J. Neurosci. Off. J. Soc. Neurosci. 37, 4481–4492.
Oldfield, R.C., 1971. The assessment and analysis of handedness: the Edinburgh inventory. Neuropsychologia 9, 97–113.
Oostenveld, R., Fries, P., Maris, E., Schoffelen, J.M., 2011. FieldTrip: open source software for advanced analysis of MEG, EEG, and invasive electrophysiological data. Comput. Intell. Neurosci. 2011, 156869.
Ozaki, I., Hashimoto, I., 2011. Exploring the physiology and function of high-frequency oscillations (HFOs) from the somatosensory cortex. Clin. Neurophysiol. Off. J. Int. Fed. Clin. Neurophysiol. 122, 1908–1923.
Ozen, S., Sirota, A., Belluscio, M.A., Anastassiou, C.A., Stark, E., Koch, C., Buzsáki, G., 2010. Transcranial electric stimulation entrains cortical neuronal populations in rats. J. Neurosci. 30, 11476–11485.
Pineda, J.A., 2005. The functional significance of mu rhythms: translating “seeing” and “hearing” into “doing. Brain Res. Brain Res. Rev. 50, 57–68.
Pozdniakov, I., Vorobiova, A.N., Galli, G., Rossi, S., Feurra, M., 2021. Online and offline effects of transcranial alternating current stimulation of the primary motor cortex. Sci. Rep. 11, 3854.
Reato, D., Rahman, A., Bikson, M., Parra, L.C., 2013. Effects of weak transcranial alternating current stimulation on brain activity-a review of known mechanisms from animal studies. Front. Hum. Neurosci. 7, 687.
Restuccia, D., Coppola, G., 2015. Auditory stimulation enhances thalamic somatosensory high-frequency oscillations in healthy humans: a neurophysiological marker of cross-sensory sensitization? Eur. J. Neurosci. 41, 1079–1085.
Restuccia, D., Valeriani, M., Grassi, E., Gentili, G., Mazza, S., Tonali, P., Mauguière, F., 2002. Contribution of GABAergic cortical circuitry in shaping somatosensory evoked scalp responses: specific changes after single-dose administration of tiagabine. Clin. Neurophysiol. Off. J. Int. Fed. Clin. Neurophysiol. 113, 656–671.
Riecke, L., Formisano, E., Herrmann, C.S., Sack, A.T., 2015. 4-Hz transcranial alternating current stimulation phase modulates hearing. Brain Stimul. 8, 777–783.
Rocchi, L., Casula, E., Tocco, P., Berardelli, A., Rothwell, J., 2016. Somatosensory temporal discrimination threshold involves inhibitory mechanisms in the primary somatosensory area. J. Neurosci. 36, 325–335.
Rogasch, N.C., Sullivan, C., Thomson, R.H., Rose, N.S., Bailey, N.W., Fitzgerald, P.B., Farzan, F., Hernandez-Pavon, J.C., 2017. Analysing concurrent transcranial magnetic stimulation and electroencephalographic data: a review and introduction to the open–source TESA software. Neuroimage 147, 934–951.
Rossi, S., Antal, A., Bestmann, S., Bikson, M., Brewer, C., Brockmöller, J., Carpenter, L.L., Cincotta, M., Chen, R., Daskalakis, J.D., et al., 2021. Safety and recommendations for TMS use in healthy subjects and patient populations, with updates on training, ethical and regulatory issues: expert guidelines. Clin. Neurophysiol. 132, 269–306.
Rossini, P.M., Babiloni, C., Babiloni, F., Ambrosini, A., Onorati, P., Carducci, F., Urbano, A, 1999. “Gating” of human short-latency somatosensory evoked cortical responses during execution of movement. A high resolution electroencephalography study. Brain Res. 843, 161–170.
Rouder, J.N., Speckman, P.L., Sun, D., Morey, R.D., Iverson, G., 2009. Bayesian t tests for accepting and rejecting the null hypothesis. Psychon. Bull. Rev. 16, 225–237.
Saito, K., Otsuru, N., Yokota, H., Inukai, Y., Miyaguchi, S., Kojima, S., Onishi, H., 2021. α-tACS over the somatosensory cortex enhances tactile spatial discrimination in healthy subjects with low alpha activity. Brain Behav 11, e02019.
Schmidt, S.L., Iyengar, A.K., Foulser, A.A., Boyle, M.R., Fröhlich, F., 2014. Endogenous cortical oscillations constrain neuromodulation by weak electric fields. Brain Stimul. 7, 878–889.
Sherman, M.A., Lee, S., Law, R., Haegens, S., Thorn, C.A., Hämäläinen, M.S., Moore, C.I., Jones, S.R., 2016. Neural mechanisms of transient neocortical beta rhythms: converging evidence from humans, computational modeling, monkeys, and mice. Proc. Natl. Acad. Sci. U. S. A. 113, E4885–E4894.
Singer, W., 2018. Neuronal oscillations: unavoidable and useful? Eur. J. Neurosci. 48, 2389–2398.
Thut, G., Schyns, P.G., Gross, J., 2011. Entrainment of perceptually relevant brain oscillations by non-invasive rhythmic stimulation of the human brain. Front. Psychol. 2, 170.
Valeriani, M., Le Pera, D, 2006. Application of dipole models in exploring somatosensory evoked potential sources. Suppl. Clin. Neurophysiol. 59, 223–231.
Valeriani, M., Restuccia, D., Di Lazzaro, V., Le Pera, D., Barba, C., Tonali, P., Mauguiere, F., 1998. Dipolar sources of the early scalp somatosensory evoked potentials to upper limb stimulation. Effect of increasing stimulus rates. Exp. Brain Res. 120, 306–315.
Vieira, P.G., Krause, M.R., Pack, C.C., 2020. tACS entrains neural activity while somatosensory input is blocked. PLOS Biol. 18, e3000834.
Vossen, A., Gross, J., Thut, G., 2015. Alpha power increase after transcranial alternating current stimulation at alpha frequency (α-tACS) reflects plastic changes rather than entrainment. Brain Stimul. 8, 499–508.
Wasaka, T., Hoshiyama, M., Nakata, H., Nishihira, Y., Kakigi, R., 2003. Gating of somatosensory evoked magnetic fields during the preparatory period of self-initiated finger movement. Neuroimage 20, 1830–1838.
Zhang, Y., Ding, M., 2010. Detection of a weak somatosensory stimulus: role of the prestimulus mu rhythm and its top-down modulation. J. Cogn. Neurosci. 22, 307–322.
Ziegler, D.A., Pritchett, D.L., Hosseini-Varnamkhasti, P., Corkin, S., Hämäläinen, M., Moore, C.I., Jones, S.R., 2010. Transformations in oscillatory activity and evoked responses in primary somatosensory cortex in middle age: a combined computational neural modeling and MEG study. Neuroimage 52, 897–912.